Mon. Not. R. Astron. Soc. **277**, 945–958 (1995)

Relative frequencies of Type Ia and Type II supernovae in the chemical evolution of the Galaxy, LMC and SMC

T. Tsujimoto,[1] K. Nomoto,[2,7] Y. Yoshii,[3,7] M. Hashimoto,[4] S. Yanagida[5] and F.-K. Thielemann[6]

[1] *National Astronomical Observatory, Mitaka, Tokyo 181, Japan*
[2] *Department of Astronomy, School of Science, University of Tokyo, Bunkyo-ku, Tokyo 113, Japan*
[3] *Institute of Astronomy, Faculty of Science, University of Tokyo, Mitaka, Tokyo 181, Japan*
[4] *Department of Physics, Faculty of Science, Kyushu University, Fukuoka 810, Japan*
[5] *Department of Earth Science, Faculty of Science, Ibaraki University, Mito, Ibaraki 310, Japan*
[6] *Institut für theoretische Physik, Universität Basel, Basel, Switzerland*
[7] *Research Center for the Early Universe, School of Science, University of Tokyo, Bunkyo-ku, Tokyo 113, Japan*

Accepted 1995 June 23. Received 1995 June 9; in original form 1993 July 23

ABSTRACT

The predicted nucleosynthesis products of Type Ia and Type II supernovae are combined with various parameter ratios and compared with the solar abundances of heavy elements and their isotopes, and also with the abundances of heavy elements in the LMC and SMC. Aided by a reasonable model of galactic chemical evolution, the ratio of the total numbers (of all time) of Type Ia to Type II supernovae that best reproduces the observed abundances is determined to be $N_{\mathrm{Ia}}/N_{\mathrm{II}}=0.15$ for the Galaxy, in agreement with current observations. For the MCs, however, this ratio is larger than that for the Galaxy, yielding $N_{\mathrm{Ia}}/N_{\mathrm{II}}=0.2$–$0.3$. We discuss several possible star formation history scenarios that may account for such an enhanced frequency of Type Ia supernovae in the MCs.

Key words: supernovae: general – galaxies: abundances – galaxies: evolution – Magellanic Clouds.

1 INTRODUCTION

Supernovae are the sites of heavy-element production in galaxies. There exist two major types of supernovae, namely Type I and Type II, and Type I supernovae are further classified into subclasses of Type Ia, Ib and Ic (e.g. Branch, Nomoto & Filippenko 1991). These different types of supernovae have different progenitors, thus producing different heavy elements on different time-scales during the chemical evolution of galaxies. We assume that stars initially more massive than 10 $M_{\odot}$ explode as Type II supernovae (SNe II) if they are single stars, or as Type Ib/Ic supernovae (SNe Ib/Ic) if they belong to close binary systems. Because the lifetime of their massive progenitors is about 10^{6-7} yr, much shorter than the age of galaxies, SNe II and SNe Ib/Ic cause heavy-element enrichment in the early phases of galactic evolution. In this paper, we associate the heavy-element yields from SNe II with those from SNe Ib/Ic.

Type Ia supernovae (SNe Ia), by contrast, produce heavy elements on a much longer time-scale, in the later phases of galactic evolution. The evolutionary time-scale of their progenitors is either related to the lifetime of the low-mass companion in a binary system, if Roche lobe overflow replenishes the white dwarf by accretion, or it depends on the initial separation of the double white dwarfs, if a merging scenario is adopted. An increasing body of data for solar neighbourhood stars has imposed a stringent constraint on the evolutionary time-scale of SN Ia progenitors, which is as long as $t_{\mathrm{Ia}}\approx 1.5$ Gyr (Yoshii, Tsujimoto & Nomoto 1995), and we adopt this value throughout this paper. For the heavy-element yields from SNe Ia, we assume that SNe Ia are a result of thermonuclear explosions of accreting white dwarfs. For details of the progenitor–supernova connection, see Branch et al. (1991).

The nucleosynthesis products of SNe Ia and SNe II and their roles in the chemical evolution of galaxies are considerably different (for a review see, e.g., Matteucci & Greggio 1986; Matteucci 1991a). The importance of treating SNe Ia separately from SNe II in modelling galactic evolution was highlighted by the fact that a reasonable mixture of the heavy-element yields from SNe Ia and SNe II is able to explain the solar abundances of heavy elements from oxygen to the iron group. The first qualitative work that demonstrated this was by Nomoto, Thielemann & Wheeler (1984a).

Yanagida, Nomoto & Hayakawa (1990), Nomoto et al. (1990) and Nomoto, Shigeyama & Tsujimoto (1991) extended this approach and obtained the ratio of SNe Ia to SNe II that reproduces the solar abundances of the possible isotopes of the elements from oxygen to nickel. In these works, the explosion model of a 25-$M_\odot$ star (Nomoto et al. 1984a) or of a 20-$M_\odot$ star (Yanagida et al. 1990; Nomoto et al. 1990, 1991) was used to represent the nucleosynthesis products of SNe II, because no extensive set of calculations for a wide range of progenitor mass was available (e.g. Artnett 1978; Woosley & Weaver 1986).

Hashimoto, Nomoto & Shigeyama (1989), Hashimoto et al. (1993a, 1994, 1995, in preparation) and Thielemann, Nomoto & Hashimoto (1990, 1994, 1995) have recently presented detailed calculations of nucleosynthesis products from SNe II for progenitor masses in the range of 13 to 70 $M_\odot$. Tsujimoto et al. (1994, 1995b) applied these results to galactic chemical evolution; particularly the mass range and slope of the initial stellar mass function (IMF), but also the iron yield from SNe II, were constrained by the solar-neighbourhood observations. Their studies enable an estimate to be made of the nucleosynthesis products of SNe II (averaged over the progenitor mass with a weighting for the IMF), and therefore a fair estimate of the ratio of SNe Ia to SNe II can be found ($N_{\rm Ia}/N_{\rm II} \sim 0.15$; see Section 3.2), which can then be compared with the observed ratio in the Galaxy (e.g. van den Bergh & Tammann 1991).

To date, similar attempts to estimate $N_{\rm Ia}/N_{\rm II}$ have been based on only a limited number of elements. For example, Arnett, Schramm & Truran (1989) used two elements (O and Fe) and obtained a slightly lower ratio than our own, $N_{\rm Ia}/N_{\rm II} \sim 1/10$, while Matteucci and her collaborators (Matteucci & François 1989; Matteucci 1991b) used eight elements (C, N, O, Ne, Mg, Si, S, Fe) and obtained a higher ratio $N_{\rm Ia}/N_{\rm II} \sim 1/4$. In obtaining these values of $N_{\rm Ia}/N_{\rm II}$, Arnett et al. and Matteucci and her collaborators fitted the abundance ratios among the elements to the observations but did not compare their individual abundances with the solar abundances as a boundary condition of the model. In this paper, however, using 14 elements as well as their isotopes and allowing for the best fit to all their solar abundances, we have obtained $N_{\rm Ia}/N_{\rm II} \sim 0.15$ for the Galaxy, which is most realistic at present.

Our method of constraining the $N_{\rm Ia}/N_{\rm II}$ ratio from an abundance pattern can also be applied to the Large and Small Magellanic Clouds (LMC and SMC), for which the observations of abundances of various heavy elements are being accumulated (e.g. Russell & Bessell 1989; Russell & Dopita 1990, 1992). We note that the abundance patterns observed for the MCs are quite different from the solar abundance pattern (see the references above, but also Pagel 1992). Matteucci (1991b) explained this difference in terms of different ratios of $N_{\rm Ia}/N_{\rm II}$ for the MCs and the Galaxy, and concluded that $N_{\rm Ia}/N_{\rm II}$ for the LMC is smaller than that for the Galaxy. Since nucleosynthesis arguments indicate that Fe is mainly produced by SNe Ia while O is mainly produced by SNe II, her conclusion seems to be the inverse of our general understanding that $N_{\rm Ia}/N_{\rm II}$ would be enhanced in the LMC because the observed O/Fe ratio for the LMC is smaller than that for the Galaxy. Under these circumstances, in Section 4.2, aided by reasonable models of chemical evolution, we have determined $N_{\rm Ia}/N_{\rm II}$ for the MCs through a comparison between the predicted and observed abundances of 10 elements for the LMC and 12 elements for the SMC. We find that $N_{\rm Ia}/N_{\rm II}$ for both the LMC and SMC is larger than for the Galaxy, in sharp contrast to Matteucci's conclusion.

2 NUCLEOSYNTHESIS PRODUCTS OF TYPE II AND TYPE IA SUPERNOVAE

Nucleosynthesis products of SNe II are those found after explosive nuclear burning by massive progenitor stars. The masses of synthesized heavy elements in 13–70 $M_\odot$ stars have been calculated (Hashimoto et al. 1989, 1993a, 1994, 1995, in preparation; Thielemann et al. 1990, 1994, 1995), and the results for various masses of progenitor stars are summarized in Table 1 (Hashimoto et al. 1995, in preparation). In the present study, we assume that the lower mass bound of the progenitors of SNe II (or the upper mass bound of the white dwarf progenitors) is $m_{\rm l} = 10\ M_\odot$ and that the heavy-element production from a star of mass $m_{\rm l}$ is negligible. In fact, the exact value of $m_{\rm l}$ strongly depends on the mass-loss rate during the AGB phase of 8–10 $M_\odot$ stars, and is thus highly uncertain, and the production of heavy elements from 8–10 $M_\odot$ stars is negligible even if these stars undergo supernova explosions (Hashimoto, Iwamoto & Nomoto 1993b).

For our later use, we define the heavy element mass, $M_{i,\rm II}$, averaged over SNe II progenitor stars with a weight of a Salpeter's IMF, that is,

$$M_{i,\rm II} = \frac{\int_{10\,M_\odot}^{m_{\rm u}} M_i(m)\, m^{-(1+x)}\, {\rm d}m}{\int_{10\,M_\odot}^{m_{\rm u}} m^{-(1+x)}\, {\rm d}m} \qquad (x=1.35), \qquad (1)$$

where $M_i(m)$ is the ith heavy-element mass produced in a star of main-sequence mass m. The upper mass limit $m_{\rm u}$ corresponds to a critical mass $m_{\rm BH}$ above which stars form black holes without ejecting heavy elements into space. Tsujimoto et al. (1994, 1995b) found that $m_{\rm BH} = 50 \pm 10\ M_\odot$ is reasonable to reproduce the break in the [O/Fe] versus [Fe/H] diagram for the solar-neighbourhood observations. Table 2 gives the average synthesized masses of 18 elements and their isotopes (a total of 42 species) for two reference values of $m_{\rm u} = 50$ and 70 $M_\odot$; the former is the best estimate of $m_{\rm BH}$ and the latter is the upper mass end of stars for which the nucleosynthesis calculations have been performed. The tabulated results are used to calculate the abundance pattern $x_i \equiv M_i/\sum_i M_i$, which is normalized to the solar $x_i(\odot) \equiv Z_i/\sum_i Z_i$, where Z_i is the observed abundance of the ith element per unit mass (Anders & Grevesse 1989). In Fig. 1 we show the normalized pattern defined as $x_i/x_i(\odot)$ for $m_{\rm u} = 50\ M_\odot$.

The nucleosynthesis products of SNe Ia are those from the carbon deflagration model W7 (Nomoto, Thielemann & Yokoi 1984b; Thielemann, Nomoto & Yokoi 1986), which has been updated with the use of the latest nuclear reaction rates (Thielemann, Nomoto & Hashimoto 1993). Table 2 gives the masses of 18 elements and their isotopes based on the updated W7 model, and Fig. 2 shows the abundance pattern normalized to solar values in the same manner as in Fig. 1. Notice that $x_{\rm O}/x_{\rm O}(\odot) \ll x_{\rm Fe}/x_{\rm Fe}(\odot)$. This clearly

Table 1. Nucleosynthesis products of SNe II for various progenitor masses.

	Synthesized isotopic mass ($M_\odot$)						
Species	m=13 $M_\odot$	m=15 $M_\odot$	m=18 $M_\odot$	m=20 $M_\odot$	m=25 $M_\odot$	m=40 $M_\odot$	m=70 $M_\odot$
^{16}O	1.51E-01	3.55E-01	7.92E-01	1.48	2.99	9.11	2.14E+01
^{18}O	9.44E-09	1.35E-02	8.67E-03	8.68E-03	6.69E-03	1.79E-06	3.80E-03
^{20}Ne	2.25E-02	2.08E-02	1.61E-01	2.29E-01	5.94E-01	6.58E-01	2.00
^{21}Ne	2.08E-04	3.93E-05	2.19E-03	3.03E-04	3.22E-03	2.36E-03	1.14E-02
^{22}Ne	1.01E-04	1.25E-02	2.74E-02	2.93E-02	3.39E-02	5.66E-02	5.23E-02
^{23}Na	7.27E-04	1.53E-04	7.25E-03	1.15E-03	1.81E-02	2.37E-02	6.98E-02
^{24}Mg	9.23E-03	3.16E-02	3.62E-02	1.47E-01	1.59E-01	3.54E-01	7.87E-01
^{25}Mg	1.38E-03	2.55E-03	7.54E-03	1.85E-02	3.92E-02	4.81E-02	1.01E-01
^{26}Mg	8.96E-04	2.03E-03	5.94E-03	1.74E-02	3.17E-02	1.07E-01	2.91E-01
^{27}Al	1.04E-03	4.01E-03	5.44E-03	1.55E-02	1.95E-02	8.05E-02	1.44E-01
^{28}Si	6.68E-02	7.16E-02	8.69E-02	8.50E-02	1.03E-01	4.29E-01	7.55E-01
^{29}Si	7.99E-04	3.25E-03	1.76E-03	9.80E-03	6.97E-03	5.43E-02	1.08E-01
^{30}Si	1.87E-03	4.04E-03	3.33E-03	7.19E-03	6.81E-03	4.32E-02	1.00E-01
^{31}P	2.95E-04	6.55E-04	4.11E-04	1.05E-03	9.02E-04	5.99E-03	2.57E-02
^{32}S	1.46E-02	3.01E-02	3.76E-02	2.29E-02	3.84E-02	1.77E-01	2.05E-01
^{33}S	1.19E-04	9.60E-05	1.48E-04	8.84E-05	2.20E-04	7.49E-04	1.02E-03
^{34}S	1.83E-03	1.49E-03	1.89E-03	1.26E-03	2.77E-03	1.14E-02	1.98E-02
^{35}Cl†	3.70E-05	3.45E-05	8.95E-05	6.05E-05	6.72E-05	4.75E-04	1.76E-03
^{37}Cl†	6.73E-06	9.60E-06	1.04E-05	4.96E-06	1.32E-05	1.17E-04	1.01E-04
^{36}Ar	2.36E-03	5.63E-03	6.13E-03	3.78E-03	6.71E-03	3.11E-02	2.92E-02
^{38}Ar	4.85E-04	6.49E-04	6.29E-04	3.25E-04	7.24E-04	9.14E-03	6.16E-03
^{39}K†	1.95E-05	3.31E-05	3.66E-05	3.24E-05	3.47E-05	3.83E-04	3.84E-04
^{41}K†	1.42E-06	2.37E-06	2.23E-06	1.28E-06	2.79E-06	3.43E-05	2.84E-05
^{40}Ca	2.53E-03	5.29E-03	5.11E-03	3.25E-03	6.15E-03	2.56E-02	2.14E-02
^{44}Ca†	1.22E-04	7.49E-05	1.43E-05	9.15E-05	2.11E-05	2.00E-05	2.97E-04
^{46}Ti†	2.56E-06	6.26E-06	6.72E-06	6.81E-06	6.84E-06	3.56E-05	1.44E-05
^{47}Ti†	5.13E-06	3.75E-06	3.11E-07	1.73E-06	9.11E-07	9.74E-07	6.26E-07
^{48}Ti†	1.68E-04	1.58E-04	8.59E-05	1.85E-04	8.98E-05	1.58E-04	1.42E-04
^{49}Ti†	3.45E-06	6.10E-06	7.54E-06	4.89E-06	6.01E-06	2.17E-05	6.97E-06
^{50}Ti†	3.56E-10	1.21E-09	1.17E-10	1.12E-10	5.90E-10	2.00E-10	2.56E-10
^{50}Cr	2.30E-05	5.15E-05	7.49E-05	3.54E-05	5.01E-05	1.49E-04	1.01E-04
^{52}Cr	1.15E-03	1.36E-03	1.44E-03	8.64E-04	1.31E-03	2.77E-03	6.86E-04
^{53}Cr	9.34E-05	1.35E-04	1.50E-04	7.12E-05	1.39E-04	3.56E-04	1.00E-04
^{54}Cr	3.35E-08	4.09E-08	2.53E-08	6.26E-09	2.41E-08	2.81E-08	7.61E-08
^{55}Mn	3.65E-04	4.74E-04	5.48E-04	2.27E-04	5.02E-04	8.41E-04	3.64E-04
^{54}Fe	2.10E-03	4.49E-03	6.04E-03	2.52E-03	4.81E-03	9.17E-03	5.81E-03
^{56}Fe	1.50E-01	1.44E-01	7.57E-02	7.32E-02	5.24E-02	7.50E-02	7.50E-02
^{57}Fe	4.86E-03	4.90E-03	2.17E-03	3.07E-03	1.16E-03	2.29E-03	3.83E-03
^{59}Co†	1.39E-04	1.22E-04	4.82E-05	1.31E-04	2.19E-05	2.51E-05	1.59E-04
^{58}Ni	5.82E-03	7.50E-03	3.08E-03	3.71E-03	1.33E-03	3.31E-03	9.25E-03
^{60}Ni	3.72E-03	3.36E-03	8.71E-04	2.18E-03	6.67E-04	3.88E-04	1.77E-03
^{62}Ni	1.05E-03	9.50E-04	2.52E-04	7.26E-04	1.70E-04	1.11E-04	1.28E-03

†These species are not used in minimizing $g(r)$ in equation (3) because of the uncertainties involved in their abundances in Type II supernovae (see Section 2).

indicates that SNe Ia enhance the iron abundance relative to oxygen during the chemical evolution of galaxies.

3 THE SOLAR ABUNDANCE PATTERN

3.1 Relative contributions of Type Ia and Type II supernovae

Let N be the total number of SNe that have ever occurred in the Galaxy, and w be the mass fraction of the synthesized elements that have been ejected from SNe and not locked up in low-mass stars. Let r be the mass fraction contributed by SNe Ia per unit mass of all heavy elements in the gas. Then we define r as

$$r = \frac{w_{\rm Ia} M_{\rm Ia} N_{\rm Ia}}{w_{\rm Ia} M_{\rm Ia} N_{\rm Ia} + w_{\rm II} M_{\rm II} N_{\rm II}}, \tag{2}$$

where $M_{\rm Ia} \equiv \sum_i M_{i,\rm Ia}$ and $M_{\rm II} \equiv \sum_{i,\rm II}$ are taken from Table 2. The abundance pattern x_i to be compared with the solar $x_i(\odot)$ is therefore written as

$$x_i = r M_{i,\rm Ia}/M_{\rm Ia} + (1-r) M_{i,\rm II}/M_{\rm II}, \tag{3}$$

and the most probable value of r is determined by minimizing the following function (Yanagida et al. 1990; Nomoto et al. 1990, 1991):

$$g(r) = \sum_{i=1}^{n} [\log x_i - \log x_i(\odot)]^2/n, \tag{4}$$

where i runs over the heavy elements and their isotopes chosen in the minimization procedure. We note that the theoretical values of x_i for some particular elements show relatively large deviations from the solar values. Some of these values would be larger if s-process nucleosynthesis products during core helium burning (Prantzos, Hashimoto & Nomoto 1990) and shell carbon burning (Raiteri et al. 1993) were included in pre-supernova evolutionary calculations (Nomoto & Hashimoto 1988). It is also the case that some odd Z elements and neutron-rich species are produced

Table 2. Nucleosynthesis products of SN II and Ia.

Species	Synthesized mass ($M_\odot$) Type II m_u=50$M_\odot$*	m_u=70$M_\odot$*	Type Ia W7
^{16}O	1.80	2.47	1.43E-01
^{18}O	4.61E-03	4.51E-03	8.25E-10
^{20}Ne	2.12E-01	2.69E-01	2.02E-03
^{21}Ne	1.08E-03	1.39E-03	8.46E-06
^{22}Ne	1.83E-02	1.99E-02	2.49E-03
^{23}Na	6.51E-03	8.56E-03	6.32E-05
^{24}Mg	8.83E-02	1.12E-01	8.50E-03
^{25}Mg	1.44E-02	1.74E-02	4.05E-05
^{26}Mg	2.01E-02	2.92E-02	3.18E-05
^{27}Al	1.48E-02	1.95E-02	9.86E-04
^{28}Si	1.05E-01	1.29E-01	1.50E-01
^{29}Si	8.99E-03	1.25E-02	8.61E-04
^{30}Si	8.05E-03	1.12E-02	1.74E-03
^{31}P	1.21E-03	1.98E-03	4.18E-04
^{32}S	3.84E-02	4.54E-02	8.41E-02
^{33}S	1.78E-04	2.11E-04	4.50E-04
^{34}S	2.62E-03	3.25E-03	1.90E-03
^{35}Cl†	1.01E-04	1.53E-04	1.34E-04
^{37}Cl†	1.88E-05	1.53E-04	3.98E-05
^{36}Ar	6.62E-03	7.67E-03	1.49E-02
^{38}Ar	1.37E-03	1.63E-03	1.06E-03
^{39}K†	6.23E-05	7.67E-05	8.52E-05
^{41}K†	5.07E-06	7.67E-05	7.44E-06
^{40}Ca	5.77E-03	6.54E-03	1.23E-02
^{44}Ca†	5.53E-05	6.14E-05	8.86E-06
^{46}Ti†	7.48E-06	1.94E-04	1.71E-05
^{47}Ti†	2.11E-06	1.94E-04	6.04E-07
^{48}Ti†	1.16E-04	1.94E-04	2.03E-04
^{49}Ti†	5.98E-06	1.94E-04	1.69E-05
^{50}Ti†	3.81E-10	1.94E-04	1.26E-05
^{50}Cr	4.64E-05	1.17E-03	2.71E-04
^{52}Cr	1.15E-03	1.17E-03	5.15E-03
^{53}Cr	1.19E-04	1.22E-04	7.85E-04
^{54}Cr	2.33E-08	1.22E-04	1.90E-04
^{55}Mn	3.86E-04	3.93E-04	8.23E-03
^{54}Fe	3.62E-03	3.77E-03	1.04E-01
^{56}Fe	8.44E-02	8.40E-02	6.13E-01
^{57}Fe	2.72E-03	2.75E-03	2.55E-02
^{59}Co†	7.27E-05	7.43E-05	1.02E-03
^{58}Ni	3.63E-03	3.78E-03	1.28E-01
^{60}Ni	1.75E-03	1.73E-03	1.05E-02
^{62}Ni	5.09E-04	5.24E-04	2.66E-03

*Average over the mass range from $m=10$ M$_\odot$ to m_u assuming a Salpeter IMF.
†These species are not used in minimizing $g(r)$ in equation (3) because of uncertainties involved in their abundances in Type II supernovae (see Section 2).

in the deepest layer of the ejecta, the amounts of which are very sensitive to the neutron excess of the very thin layer, and are therefore subject to large uncertainties. (For a more detailed discussion, see Hashimoto et al. 1993a, 1994; Thielemann et al. 1993, 1995.) The isotopes of these elements are shown by open circles in Figs 1 and 3 and are not used in the minimization procedure.

Theoretical values of $M_{i,\mathrm{Ia}}$ and $M_{i,\mathrm{II}}$ for $m_u=50$ M$_\odot$ in Table 2 are taken as a standard input and are used to reproduce the solar abundance pattern (Anders & Grevesse 1989) for 14 elements (O, Ne, Na, Mg, Ar, Si, P, S, Ar, Ca, Cr, Mn, Fe, Ni) and their isotopes (a total of 31 species). Fig. 3 shows the normalized abundance pattern $x_i/x_i(\odot)$ calculated from equation (3) with the most probable value $r=r_p=0.09$, and in the inset of this figure $g(r)$ is plotted as a sequence of r. The contribution of SNe Ia to each element abundance is written as

$$r_i=\frac{r_p M_{i,\mathrm{Ia}}/M_{\mathrm{Ia}}}{r_p M_{i,\mathrm{Ia}}/M_{\mathrm{Ia}}+(1-r_p)M_{i,\mathrm{II}}/M_{\mathrm{II}}}, \tag{5}$$

and is tabulated in Table 3.

Using $M_{i,\mathrm{II}}$ for $m_u=70$ M$_\odot$ as another input, we have found that the most probable value of r in this case is $r_p=0.10$, and that it is very insensitive to the upper mass limit as far as $m_u \gtrsim 30$ M$_\odot$. The value of r_p does not depend on m_l, because heavy-element production from 8- to 10-M$_\odot$ stars is negligible, so that $M_{i,\mathrm{II}}/M_{\mathrm{II}}$ in equation (3) does not depend on m_l. We examined how r_p depends on our choice of elements. By adding the isotopic abundances of each of the 14 elements chosen, we obtained $r_p=0.08$ as the most probable value. The resulting abundance pattern $x_i/x_i(\odot)$, in this case with $r_p=0.08$, is shown in Fig. 4, together with the function $g(r)$ in the inset. Furthermore, we repeated the calculations for different IMF slopes and found that changing the slope index from $x=0.5$ to 2 changes r_p by less than 10 per cent only. Thus, considering the standard model and its variants above, the value of r_p is constrained to be $r_p=0.09\pm0.01$ against possible uncertainties in the analysis.

Using the r_p thus obtained, and taking M_{Ia} and M_{II} from Table 2, we can estimate the relative frequency of occurrence of SNe Ia and SNe II from equation (2):

$$\frac{w_{\mathrm{Ia}}N_{\mathrm{Ia}}}{w_{\mathrm{II}}N_{\mathrm{II}}}=\frac{r_p M_{\mathrm{II}}}{(1-r_p)M_{\mathrm{Ia}}}=0.184, \tag{6}$$

where w_{Ia} and w_{II} represent the mass fraction of heavy elements ejected into the interstellar gas from SNe Ia and SNe II, respectively. Assuming that this fraction is not selective among ejected elements and remembering that the oxygen and iron are mostly produced by SNe II and SNe Ia, respectively, we write

$$w_{\mathrm{II}}=\frac{f_g Z_{g,\mathrm{O}}}{(1-f_g)Z_{s,\mathrm{O}}+f_g Z_{g,\mathrm{O}}}, \tag{7}$$

and

$$w_{\mathrm{Ia}}=\frac{f_g c_g Z_{g,\mathrm{Fe}}}{(1-f_g)c_s Z_{s,\mathrm{Fe}}+f_g c_g Z_{g,\mathrm{Fe}}}, \tag{8}$$

where f_g and $1-f_g$ are the mass fractions of the interstellar gas and of stars, respectively. Here, Z_g is the present heavy-element abundance in unit mass of the gas, and Z_s is the heavy-element abundance averaged over the present metallicity distribution of stars. In equation (8) the factor c is introduced to correct for the non-negligible SN II contribution to the iron abundance. This contribution is estimated from the O/Fe ratio for metal-poor stars, because their O and Fe abundances exhibit genuine products of SNe II. Now, the correction factor is written as

$$c_g=1-10^{-[\mathrm{O/Fe}]_{\mathrm{II}}}(Z_{\mathrm{O}}/Z_{\mathrm{Fe}})_g/(Z_{\mathrm{O}}/Z_{\mathrm{Fe}})_\odot,$$

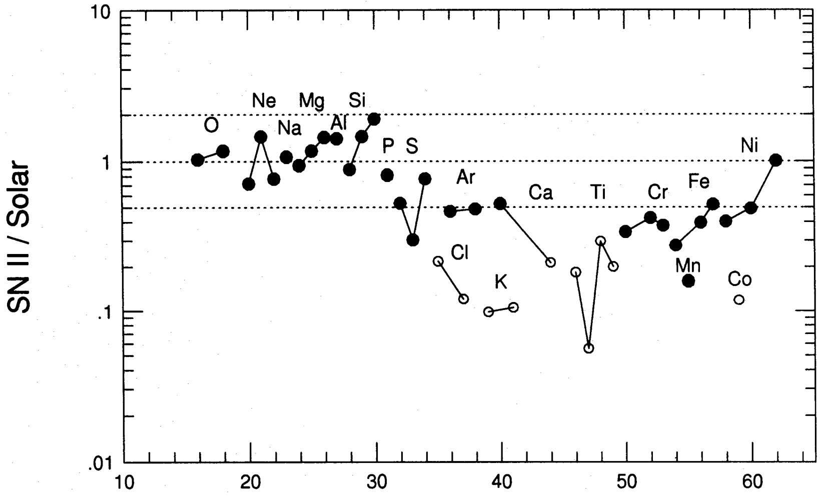

Figure 1. Abundance pattern from Type II supernova explosions. Relative abundances of synthesized heavy elements and their isotopes, normalized to the corresponding solar abundances, $x_i/x_i(\odot)$, are shown by circles. The species indicated by open circles are not used in minimizing $g(r)$ in equation (3), because of uncertainties involved in their abundances in Type II supernovae (see Section 2).

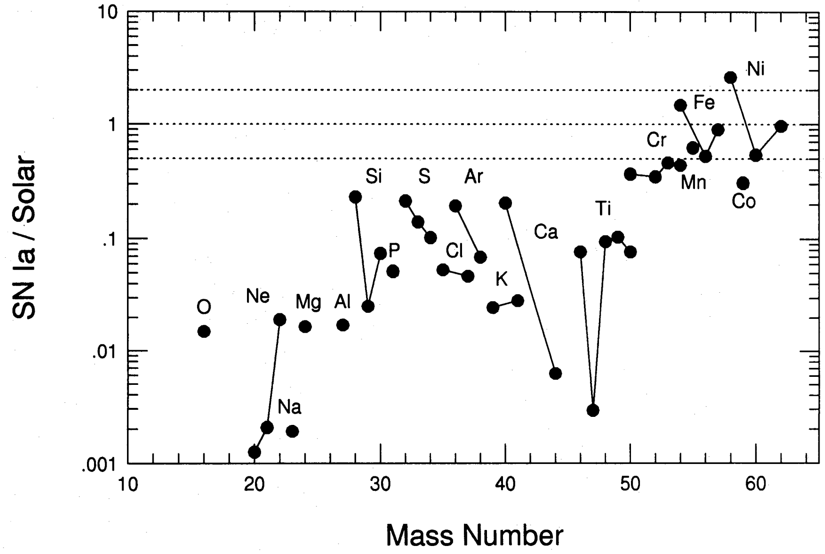

Figure 2. Abundance pattern from Type Ia supernova explosions. The relative abundances of synthesized heavy elements and their isotopes, normalized to the corresponding solar abundances, $x_i/x_i(\odot)$, are shown by circles.

or

$$c_s = 1 - 10^{-[\mathrm{O/Fe}]_{\mathrm{II}}} (Z_{\mathrm{O}}/Z_{\mathrm{Fe}})_s / (Z_{\mathrm{O}}/Z_{\mathrm{Fe}})_{\odot}, \qquad (9)$$

where $[\mathrm{O/Fe}]_{\mathrm{II}}$ stands for the observed oxygen excess relative to iron for metal-poor stars with $[\mathrm{Fe/H}] \lesssim -1$.

It is apparent from equations (7) and (8) that w_{Ia} and w_{II} depend on the star formation history. If star formation occurs continuously in the solar neighbourhood (Gallagher, Hunter & Tutukov 1984), we would expect that $w_{\mathrm{Ia}} \sim w_{\mathrm{II}}$. If the star formation rate is not constant over the age of the Galaxy and has a peak as inferred from the metallicity distribution of solar-neighbourhood G dwarfs, the efficiency w_{Ia} might be slightly larger than w_{II}. This naive argument gives a rough estimate of $N_{\mathrm{Ia}}/N_{\mathrm{II}} \lesssim 0.184$. Precise estimates of $w_{\mathrm{Ia}}/w_{\mathrm{II}}$, and therefore of $N_{\mathrm{Ia}}/N_{\mathrm{II}}$, need models of galactic chemical evolution, as we discuss below.

3.2 Chemical evolution model for the solar neighbourhood

We have made a simplified model of chemical evolution which is fairly standard, allowing material inflow from outside the considered zone (cf. Tinsley 1980). Technical details of the model are discussed fully in a separate paper (Yoshii et al. 1995) and we do not repeat them here. Among the input parameters summarized in Table 4, the time-scale t_{fall} of infall, the lifetime t_{Ia} of SN Ia progenitors, the power-

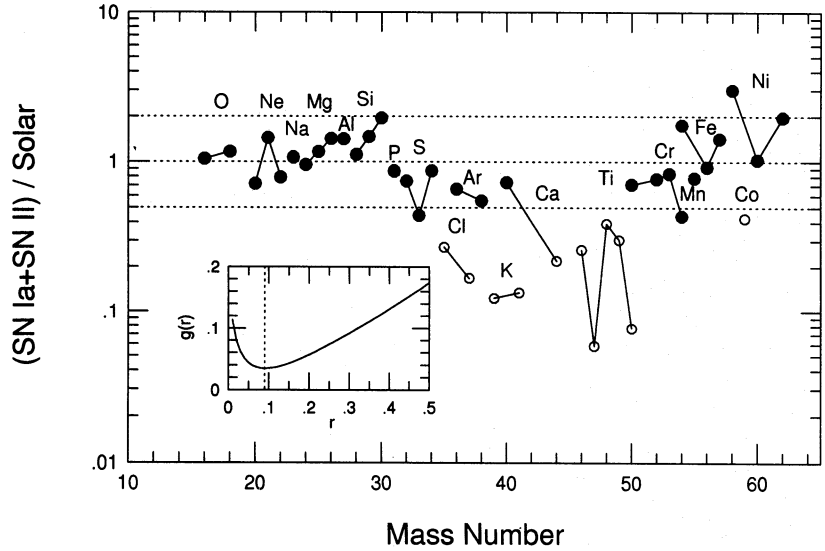

Figure 3. Solar abundance pattern based on synthesized heavy elements, from a composite of Type Ia and Type II supernova explosions with the most probable rato of r_p. The relative abundances of synthesized heavy elements and their isotopes, normalized to the corresponding solar abundances, $x_i/x_i(\odot)$, are shown by circles. The species indicated by open circles are not used in minimizing $g(r)$ in equation (3), because of uncertainties involved in their abundances in Type II supernovae (see Section 2). The inset shows the minimizing function $g(r)$ for which $r_p = 0.09$.

Table 3. Relative contribution of SN Ia to the abundance of each species.

	r_i			
	Solar Neighborhood		LMC	SMC
element (i)	r_p=0.09	r_p=0.08	r_p=0.16	r_p=0.19
O	0.01/0.00	0.01	0.03	0.03
Ne	0.00/0.00/0.02	0.00	0.01	0.01
Na	0.00	0.00		0.00
Mg	0.02/0.00/0.00	0.01	0.03	0.03
Al	0.01	0.01		
Si	0.21/0.02/0.04	0.17		0.35
P	0.06	0.05		
S	0.29/0.32/0.12	0.25	0.44	0.48
Ar	0.29/0.12	0.24	0.43	0.46
Ca	0.28	0.25	0.44	0.48
Cr	0.45/0.45/0.55/0.55	0.44	0.65	0.68
Mn	0.80	0.77	0.89	0.90
Fe	0.84/0.57/0.63	0.57	0.76	0.78
Ni	0.87/0.52/0.49	0.79	0.90	0.91

Note. The results for isotopic abundances are shown in the second column; otherwise, only results for element abundances are given.

law index k of the star formation rate, and the present O and Fe abundances in the gas, $Z_{g,O}$ and $Z_{g,Fe}$, are adjusted to reproduce the break in the [O/Fe] versus [Fe/H] diagram (Fig. 5a) and the metallicity distribution of solar-neighbourhood G dwarfs (Fig. 5c). On the other hand, the present mass fraction f_g of gas is taken from Young & Scoville (1991), and the oxygen excess $[O/Fe]_{II}$ for metal-poor stars is taken from various references (Fig. 5a).

Using these input parameters, we calculate the evolutionary behaviour of O and Fe abundances in the gas and stars. The calculated quantities relevant to our discussion are given in Table 4 and the features of the model are shown in Figs 5(a)–(d). The model O and Fe distributions of stars (Figs 5c and d) can be used to compute the stellar average O and Fe abundances, $Z_{s,O}$ and $Z_{s,Fe}$, and then w_{Ia} and w_{II} can be obtained from equations (6) and (7). We have confirmed from the model that w_{Ia} is slightly larger than w_{II}, and we obtain, finally, $N_{Ia}/N_{II} = 0.15$. This ratio would be slightly smaller if m_l were smaller than 10 $M_\odot$, due to the different normalization in M_{II} according to equations (1) and (6). For example, if $m_l = 8\ M_\odot$, the ratio would be $N_{Ia}/N_{II} = 0.15 \times (8/10)^{1.35} = 0.11$. We note that this is the ratio between the total numbers of SNe Ia and SNe II that have ever occurred in the Galaxy. If the star formation rate were almost constant, as in the solar neighbourhood, the number ratio obtained here would be close to the ratio of the SNe Ia to SNe II (and the associated SNe Ib/Ic) occurence rates in the recent past. Analyses of the observed rates of supernova explosions give $\dot{N}_{Ia}/\dot{N}_{II/Ib/Ic} \sim 0.15$ (van den Bergh & Tammann 1991) and $\sim$ 0.10 in Sbc–Sc galaxies (Tammann 1993), in good agreement with our estimate based on the nucleosynthesis arguments.

4 THE LMC AND SMC ABUNDANCE PATTERNS

4.1 Relative contributions of Type Ia and II supernovae

Fig. 6 shows a summary of the observed abundances of heavy elements in the LMC and SMC compiled by Russell & Dopita (1992). The heavy-element abundances for the MCs are deficient by a factor of 2–4 relative to their solar abundances. The MC abundance patterns are also different from the solar abundance pattern; for example, the O/Fe ratio in the MCs is smaller than the solar ratio. As the O production is dominated by SNe II and Fe production is dominated by SNe Ia, the different O/Fe ratio suggests a different relative frequency between these types of supernovae.

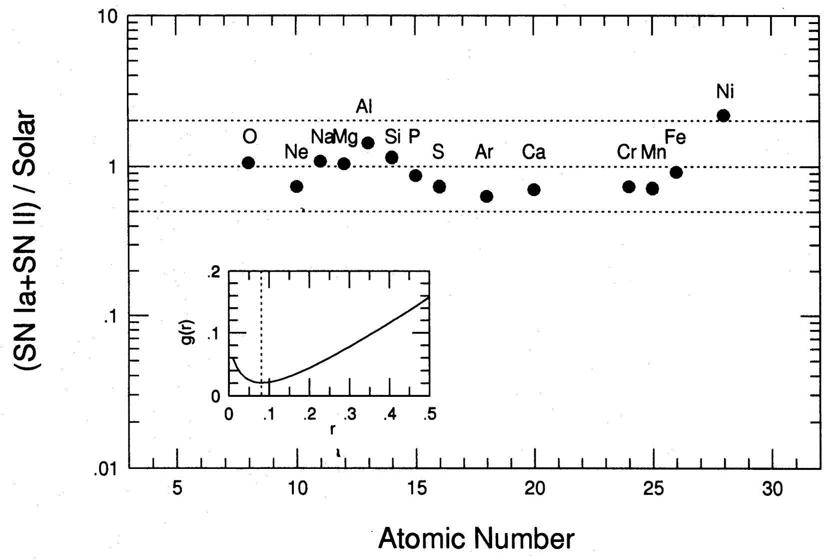

Figure 4. Solar abundance pattern based on synthesized heavy elements, from a composite of Type Ia and Type II supernova explosions with the most probable ratio of r_p. As Fig. 2, but for the abundances of heavy elements by adding their isotopic abundances and $r_p = 0.08$.

Table 4. The input parameters and calculated quantities in the chemical evolution models for the solar neighbourhood, LMC and SMC.

		continuous model			burst model	
		Solar Neighborhood	LMC	SMC	LMC	SMC
input parameters...........	t_{fall}	5	5	5	0.3	0.3
	t_{Ia}	1.5	1.5	1.5	1.5	1.5
	k	1	1	1	1	1
	f_g	0.15	0.15	0.36	0.15	0.36
	$[O/Fe]_{II}$	0.41	0.31	0.27	0.34	0.28
	$[O/H]_g$	0.0	-0.58	-0.90	-0.58	-0.90
	$[Fe/H]_g$	0.1	-0.28	-0.67	-0.28	-0.67
	t_1–t_2	...	...	...	1–12	1–12
calculated quantities	$[O/H]_s$	-0.20	-0.78	-1.16	-1.44	-1.64
	$[Fe/H]_s$	-0.17	-0.56	-0.98	-1.52	-1.71
	w_{Ia}	0.27	0.26	0.55	0.82	0.90
	w_{II}	0.22	0.22	0.50	0.56	0.76
	x	1.35*	1.73	1.88	1.62	1.84
	N_{Ia}/N_{II}	0.15	0.24	0.30	0.21	0.28

Note. t_{fall}, t_{Ia}, t_1 and t_2 are in units of Gyr. In the burst models, star formation between t_1 and t_2 has been stopped.
* This value is the input parameter.

We adopt $M_{i,\mathrm{II}}$ for $m_u = 50\ \mathrm{M}_\odot$ from Table 2 as a standard input of SN II products by adding the isotropic abundances of each of the elements. As in Section 3.1, we minimize the function $g(r)$ and reproduce the MC abundance patterns, x_i(LMC) for 10 elements (O, Ne, Mg, S, Ar, Ca, Cr, Mn, Fe, Ni) and x_i(SMC) for 12 elements (O, Ne, Na, Mg, Si, S, Ar, Ca, Cr, Mn, Fe, Ni).

Fig. 7 shows the fitted abundance pattern for the LMC, with the most probable value $r_p = 0.16$, and Fig. 8 shows the same for the SMC, with $r_p = 0.19$. Although the IMF is not used to obtain r_p (Section 3.1), the relative frequency $w_{Ia}N_{Ia}/w_{II}N_{II}$ depends on the IMF parameters through the definition of M_{II} in equation (1). Until we discuss the IMF for the MCs in Section 4.3, we retain such an IMF dependence of M_{II} in $w_{Ia}N_{Ia}/w_{II}N_{II}$ by introducing the quantity γ, which is of order unity:

$$\gamma = \frac{M_{II}(m_u, x)}{M_{II}(50\ \mathrm{M}_\odot, 1.35)}, \qquad (10)$$

where the denominator is based on our standard input for the solar neighbourhood analysis. Substituting r_p and γ into equation (5), we obtain $w_{Ia}N_{Ia}/w_{II}N_{II} = 0.52\gamma$ for the LMC and $w_{Ia}N_{Ia}/w_{II}N_{II} = 0.65\gamma$ for the SMC. Apparently, these ratios for the MCs are significantly larger than $w_{Ia}N_{Ia}/w_{II}N_{II} = 0.184$ for the Galaxy, being larger for more metal-deficient irregular galaxies. This is explained by either the occurrence frequency of SNe Ia or the ejection efficiency of heavy ele-

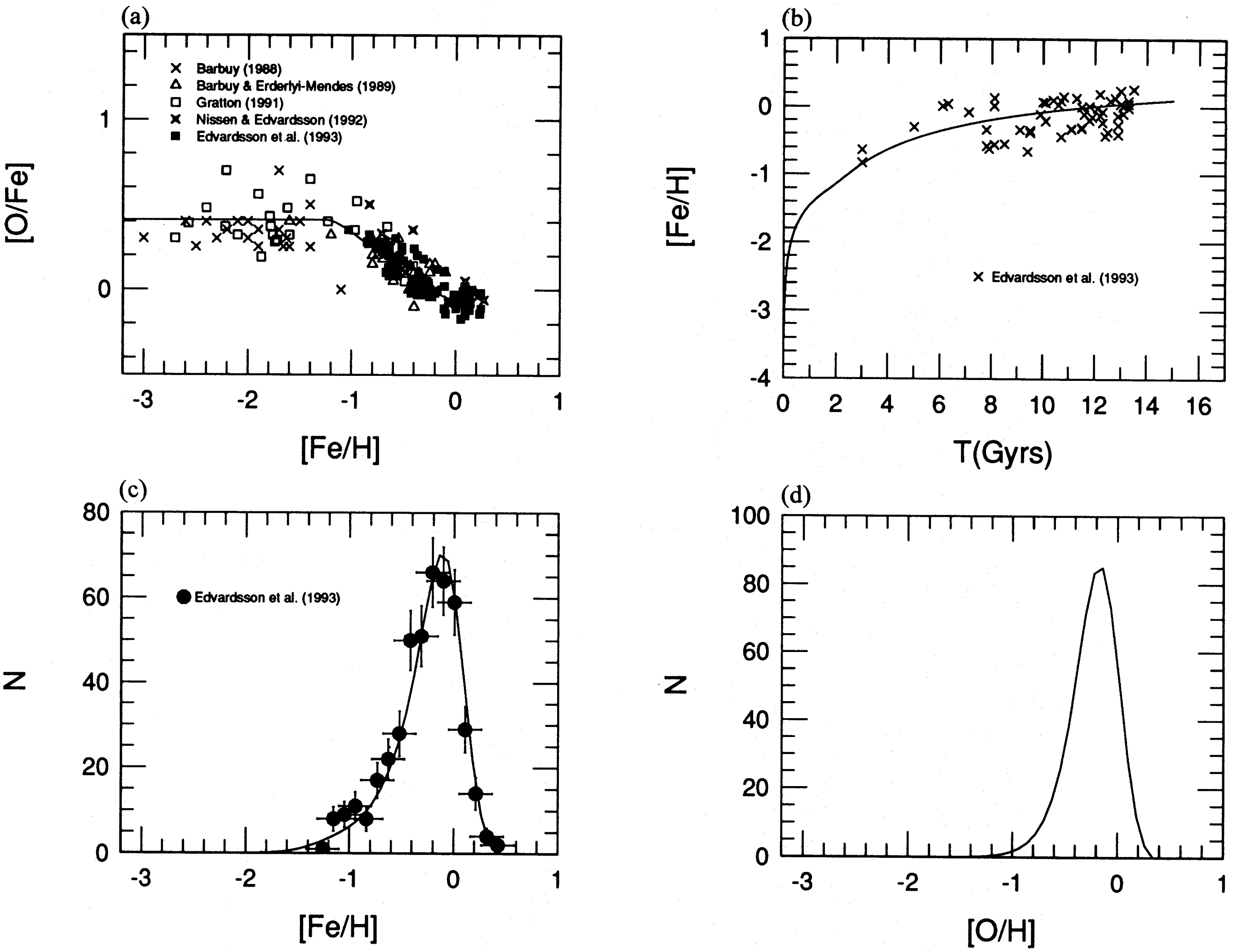

Figure 5. Chemical features for the solar neighbourhood: (a) the [O/Fe] versus [Fe/H] diagram; (b) the age–metallicity relation, (c) the present Fe distribution of stars, and (d) the present O distribution of stars. The model results are shown by thick lines and the data by symbols. The total number of stars is adjusted to agree with the number of Edvardsson et al.'s stars in their [Fe/H] sample.

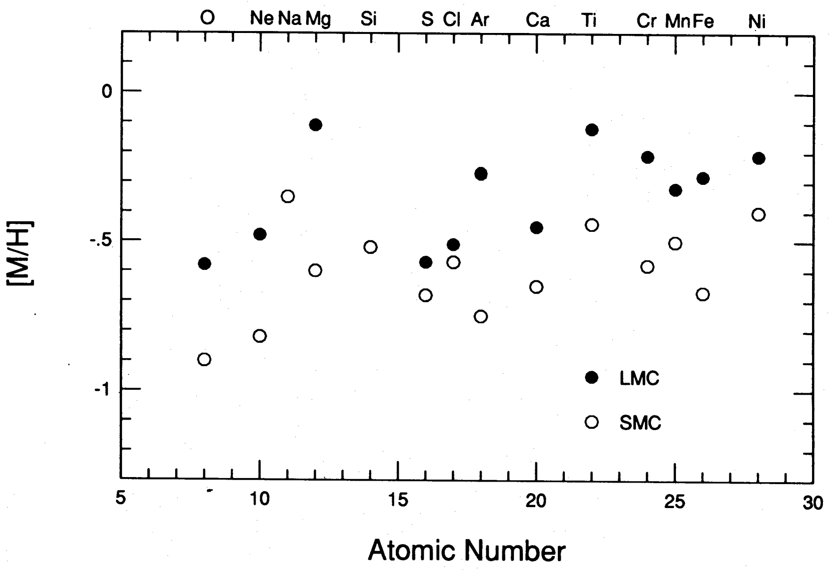

Figure 6. Abundances of LMC and SMC heavy elements relative to their corresponding solar abundances; $[M/H]_i \equiv \log(M/H)_i - \log(M/H)_{i\odot}$.

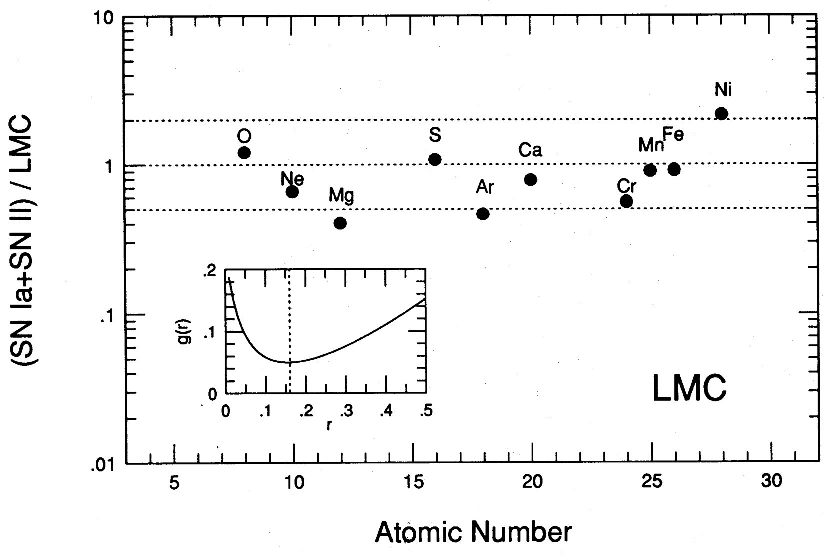

Figure 7. LMC abundance pattern based on synthesized heavy elements, from a composite of Type Ia and Type II supernova explosions with the most probable ratio of r_p. The relative abundances of synthesized heavy elements, normalized to the observed abundances, x_i/x_i(LMC), are shown by circles. The inset shows the minimizing function $g(r)$ for which $r_p = 0.16$.

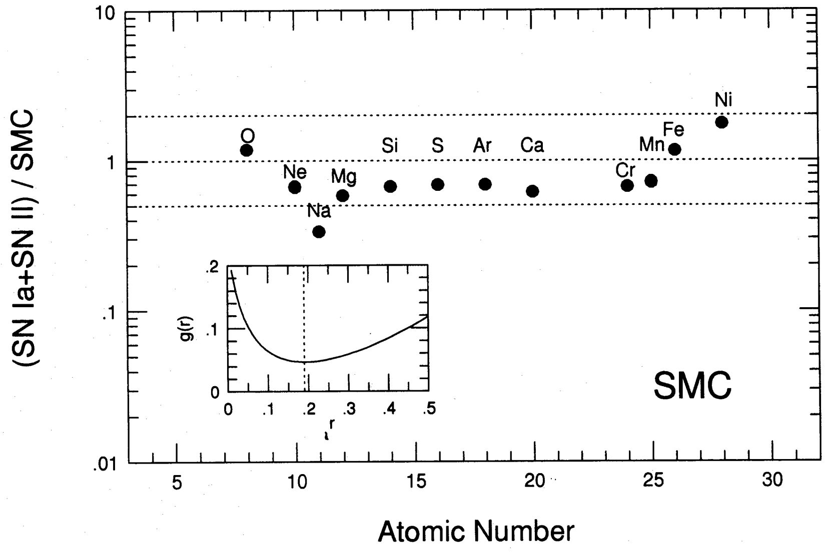

Figure 8. SMC abundance pattern based on synthesized heavy elements, from a composite of Type Ia and Type II supernova explosions with the most probable ratio of r_p. As Fig. 7, but for x_i/x_i(SMC) and $r_p = 0.19$.

ments from SNe Ia, both being enhanced relative to SNe II in the MCs.

4.2 Chemical evolution models for the LMC and SMC

The ejection efficiencies $w_{\rm Ia}$ and $w_{\rm II}$ depend on the star formation history. Gilmore & Wyse (1991) discussed the effects of starburst on the chemical evolution of the MCs.

If the MCs undergo a starburst for a period that is shorter than the lifetime of SN Ia progenitors, the elements from SNe II are produced on a similar time-scale to the burst, while the elements from SNe Ia are continuously released on a time-scale much longer than the burst period. Thus, in the post-burst phase, after stars start to explode as SNe Ia, the O/Fe ratio is significantly decreased, and therefore $w_{\rm Ia}/w_{\rm II}$ is increased.

The observed age–metallicity relations for the LMC and SMC star clusters (Da Costa 1990) can provide information as to whether stellar populations are formed continuously or as a burst. The fact that there is only one LMC cluster between 3 and 13 Gyr might support the idea of a starburst in this galaxy. However, the lack of clusters in this period could simply be a selection effect, and it is also possible that the formation of stars has little connection with the formation of star clusters. On the other hand, the ages of SMC clusters are spread over a wide range without any gap, which is suggestive of a continuous formation of clusters. Since it is premature from current observations to distinguish between continuous star formation and an initial starburst, we consider these two different views of the star formation history in this section.

The input parameters and the calculated quantities for the LMC and SMC are summarized in Table 4. The results of continuous star formation are shown by dotted lines, and those of a starburst by thick lines, in Figs 9(a)–(d) for the LMC and in Figs 10(a)–(d) for the SMC. For a continuous star formation model, the general behaviour of the chemical evolution of the MCs is similar to the solar-neighbourhood evolution, except that the present abundances of heavy elements in the MCs are smaller than solar. The ratios of $w_{\rm IA}/w_{\rm II}$ for the MCs are equally close to unity, leading to $N_{\rm Ia}/N_{\rm II}=0.32\gamma$ for the LMC and $N_{\rm Ia}/N_{\rm II}=0.39\gamma$ for the SMC. These ratios should be multiplied by $(8/10)^{1.35}=0.74$ when $m_{\rm l}=8\ {\rm M}_{\odot}$.

For a starburst model, we have assumed that an initial burst occurs from the epoch of galaxy formation, with a duration of 1 Gyr, and that a quiescent phase of negligible star formation continues until the last 3 Gyr. In this case, $w_{\rm Ia}$ and $w_{\rm II}$ for the MCs are larger than for the continuous star formation model. As the ejected elements from SNe are ineffectively locked in stars, the average stellar metallicities of O and Fe become very low and a break appears, corresponding to a quiescent phase of negligible star formation (see the thick lines in Figs 9c and d and Figs 10c and d). Moreover, the ratios of $w_{\rm Ia}/w_{\rm II}$ for the MCs are also larger than those from the continuous star formation model. This effect is understood as follows. The heavy elements ejected from SNe II during the initial burst are largely trapped in stars and a small fraction of the heavy elements is contained in the gas. On the other hand, as SNe Ia start to occur after $t\sim t_{\rm Ia}(\approx 1.5$ Gyr; Tsujimoto et al. 1995a, in preparation), the heavy elements ejected from SNe Ia are restored in the gas because of the absence of star formation. After several Gyr, the gas becomes considerably enriched with Fe and SNe Ia, which obviously lowers the O/Fe ratio. Using the derived ratios of $w_{\rm Ia}/w_{\rm II}$ for the MCs, we obtain $N_{\rm Ia}/N_{\rm II}=0.26\gamma$ for the LMC, and $N_{\rm Ia}/N_{\rm II}=0.37\gamma$ for the SMC. These ratios should be multiplied by $(8/10)^{1.35}=0.74$ when $m_{\rm l}=8\ {\rm M}_{\odot}$.

We point out that $N_{\rm Ia}/N_{\rm II}$ could be further decreased if the intial starburst develops a galactic wind and a large part of

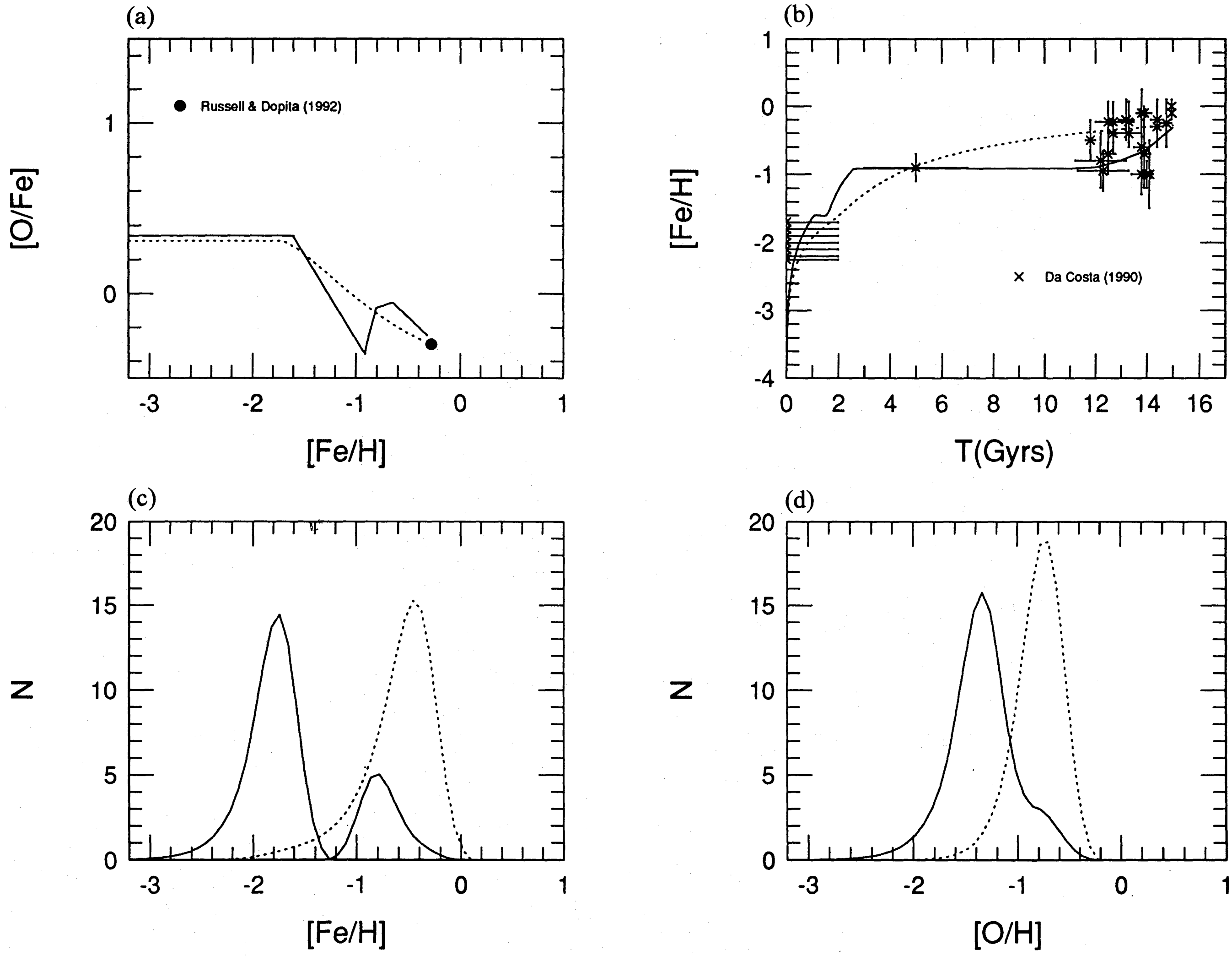

Figure 9. Chemical evolution features for the LMC: (a) the [O/Fe] versus [Fe/H] diagram; (b) the age–metallicity relation; (c) the present Fe distribution of stars, and (d) the present O distribution of stars. The model results are shown by thick lines and the data by symbols. The total number of stars is normalized to 100, because no such data are available to date.

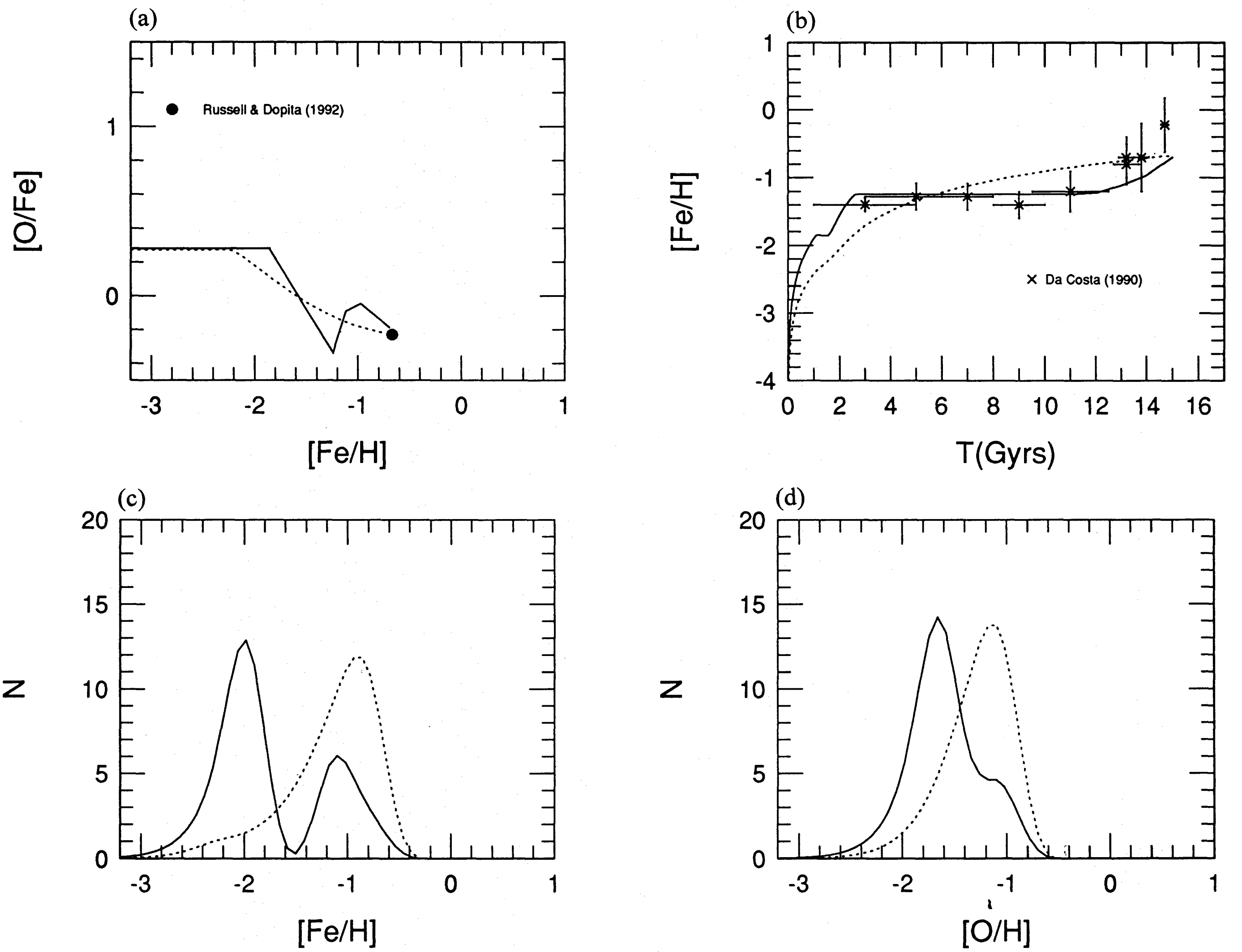

Figure 10. Chemical evolution features. As Fig. 9, but for the SMC.

the heavy elements from SNe II are removed from the galaxy. It is therefore interesting to investigate whether a reasonable wind model for the MCs predicts a value of $N_{\rm Ia}/N_{\rm II}$ that is as small as the ratio obtained for the solar neighbourhood in Section 3.2.

4.3 IMFs for the LMC and SMC

Nucleosynthesis arguments indicate that the comparison between the predicted and observed abundance patterns determines $r_{\rm p}$, and therefore $w_{\rm Ia}N_{\rm Ia}M_{\rm Ia}/w_{\rm II}N_{\rm II}M_{\rm II}[\equiv r_{\rm p}/(1-r_{\rm p})]$, almost irrespective of the IMF parameters (see Section 3.1). In addition, chemical evolution models are usually contrived to determine the heavy-element yields that reproduce the observed chemical abundances of the gas and stars, so that $w_{\rm Ia}$ and $w_{\rm II}$ can be determined without knowing the IMF parameters in advance. Consequently, the product of $N_{\rm Ia}/N_{\rm II}$ and $M_{\rm Ia}/M_{\rm II}$ has also been obtained without explicitly using the IMF.

On the other hand, $N_{\rm Ia}/N_{\rm II}$ and $M_{\rm Ia}/M_{\rm II}$ are expressed in terms of the IMF ignoring the lifetimes of supernova progenitors, as

$$\frac{N_{\rm Ia}}{N_{\rm II}}=\frac{A\int_{3\,{\rm M}_\odot}^{8\,{\rm M}_\odot} m^{-(1+x)}\,{\rm d}m}{\int_{10\,{\rm M}_\odot}^{m_{\rm u}} m^{-(1+x)}\,{\rm d}m} \tag{11}$$

and

$$\frac{M_{\rm Ia}}{M_{\rm II}}=\frac{M_{\rm Ia}\int_{10\,{\rm M}_\odot}^{m_{\rm u}} m^{-(1+x)}\,{\rm d}m}{\sum_i\int_{10\,{\rm M}_\odot}^{m_{\rm u}} M_i(m)\,m^{-(1+x)}\,{\rm d}m}, \tag{12}$$

where A denotes the mass fraction of 3–8 M$_\odot$ stars that are born as binaries of that particular breed that eventually produce SNe Ia. Using a Salpeter IMF ($x=1.35$) and $m_{\rm u}=m_{\rm BH}=50$ M$_\odot$ together with $N_{\rm Ia}/N_{\rm II}=0.15$ for the solar neighbourhood (Section 3.2), we obtain $A=0.036$ from equation (11). Since there is no compelling evidence that A changes by much from galaxy to galaxy, we assume that

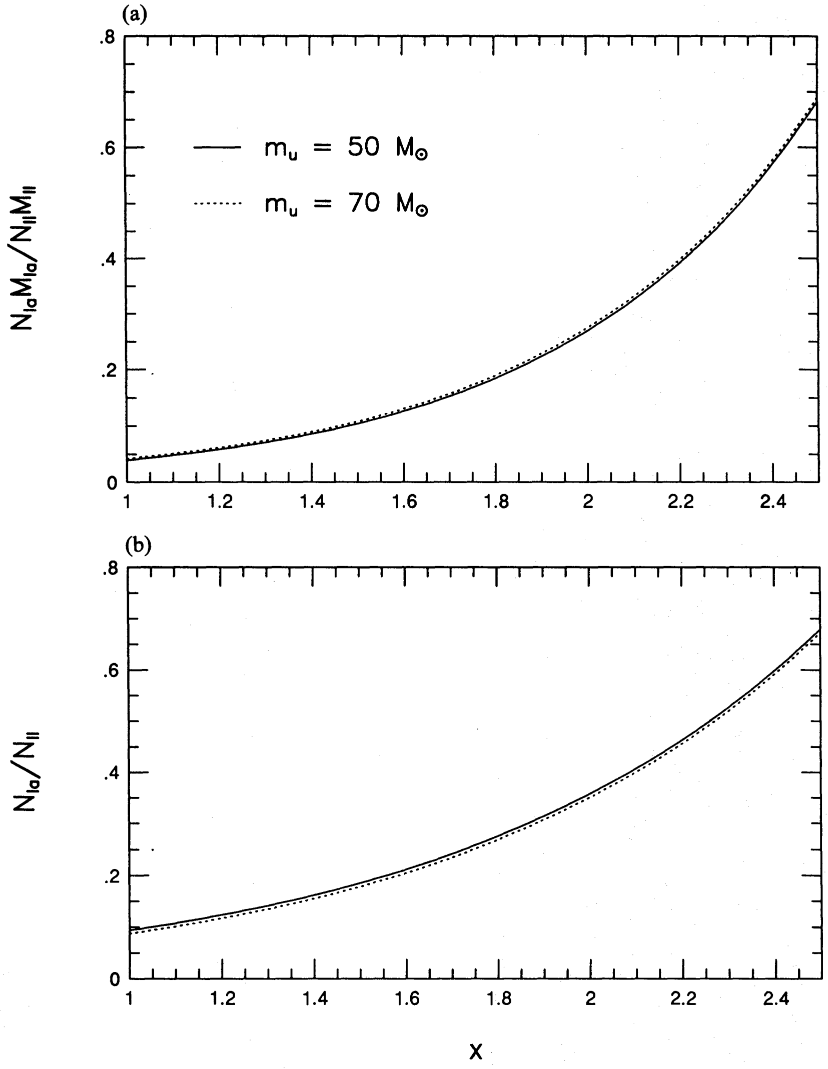

Figure 11. Ratios of various quantities of Type Ia to Type II supernovae as a function of the IMF slope index x: (a) the $(N_{\rm Ia}M_{\rm Ia}/N_{\rm II}M_{\rm II})$–$x$ relation, and (b) the $(N_{\rm Ia}/N_{\rm II})$–x relation.

$A=0.036$ holds for the MCs as well. [$N_{\rm Ia}M_{\rm Ia}/N_{\rm II}M_{\rm II}$, which we obtained in the previous section, does not depend on $m_{\rm l}$, so that A does not depend on $m_{\rm l}$ either, as seen from equations (11) and (12).]

We show the $(N_{\rm Ia}M_{\rm Ia}/N_{\rm II}M_{\rm II})$–$x$ relation in Fig. 11(a) and the $(N_{\rm Ia}/N_{\rm II})-x$ relation in Fig. 11(b), for $m_{\rm u}=50$ and 70 $\rm M_\odot$. Using the $(N_{\rm Ia}M_{\rm Ia}/N_{\rm II}M_{\rm II})$–$x$ relation, the IMF slope index x corresponding to the ratio $N_{\rm Ia}M_{\rm Ia}/N_{\rm II}M_{\rm II}$ obtained in the previous section is evaluated and is used to obtain the relative frequency $N_{\rm Ia}/N_{\rm II}$ from the $(N_{\rm Ia}/N_{\rm II})$–x relation. For the LMC, the results of $x=1.71$ (continuous) and 1.62 (burst) lead to $N_{\rm Ia}/N_{\rm II}=0.24$ and 0.21, respectively. Similarly, for the SMC, $x=1.88$ (continuous) and 1.84 (burst) lead to $N_{\rm Ia}/N_{\rm II}=0.30$ and 0.28, respectively. (If $m_{\rm l}=8$ $\rm M_\odot$ is used instead of 10 $\rm M_\odot$, these ratios would be smaller by a factor of ~1.5, but the slope x does not depend on $m_{\rm l}$.) We should note that a significant galactic wind after a starburst could lead to smaller $N_{\rm Ia}/N_{\rm II}$ and thus a shallower slope x than those in Table 4.

The IMF slopes thus derived are used to predict the oxygen excess $\rm [O/Fe]_{II}$ for metal-poor stars in the MCs. We show the $\rm [O/Fe]_{II}$–x relation for $m_{\rm u}=50$ and 70 $\rm M_\odot$ in Fig. 12(a), and the $\rm [O/Fe]_{II}$–$m_{\rm u}$ relation for $x=1.35$ and 2.0 in Fig. 12(b). Given the IMF slope index x for the MCs, the corresponding $\rm [O/Fe]_{II}$ depends slightly on the upper mass limit $m_{\rm u}$ of the IMF. A standard input of $m_{\rm u}=50\pm10$ $\rm M_\odot$ (Tsujimoto et al. 1994, 1995) in this paper gives a value of $\rm [O/Fe]_{II}$ that is as small as ~0.3. As there are no such data for the MCs, we have iteratively searched for the appropriate value of $\rm [O/Fe]_{II}$ that becomes consistent with the presumed IMF slope in chemical evolution calculations. The values searched for $\rm [O/Fe]_{II}$ are tabulated in Table 4 as the input of the model.

5 CONCLUSION

We have determined the ratio of the total numbers (of all time) of Type Ia to Type II supernovae that best reproduces the solar abundances of heavy elements and those observed for the Large and Small Magellanic Clouds. Uncorrected for the fraction of heavy elements ejected into the interstellar gas

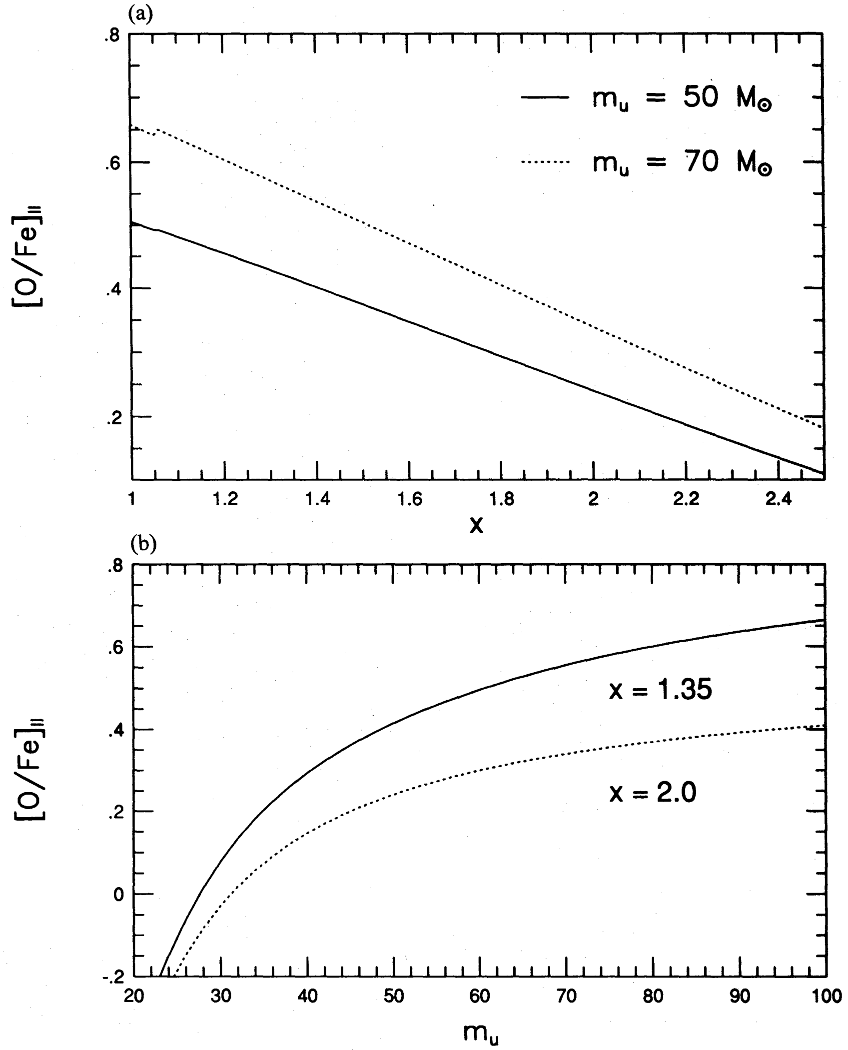

Figure 12. Oxygen excess relative to iron for metal-poor stars, $[O/Fe]_{II}$, as a function of (a) the slope index x of the IMF, and (b) the upper mass limit m_u of the IMF.

from supernovae, this ratio is found to be $w_{Ia}N_{Ia}/w_{II}N_{II} = 0.184$ for the solar neighbourhood, whereas it is as large as 0.52γ (for the LMC) and 0.65γ (for the SMC), where γ is a quantity of order unity (for details see Section 4.1).

The ratio of ejection efficiencies w_{Ia}/w_{II} is directly connected to the star formation history in a galaxy. In order to make a precise estimate of w_{Ia}/w_{II}, we have made a reasonable model of chemical evolution, taking explicitly into account the heavy-element yields from Type Ia and Type II supernova explosions. From the calculated ratio of w_{Ia}/w_{II}, the relative frequency of Type Ia to Type II supernovae is $N_{Ia}/N_{II} = 0.15$ for the solar neighbourhood, in good agreement with the observational estimate by van den Bergh & Tammann (1991).

For the MCs, however, the relative frequency of Type Ia to Type II supernovae is larger than that for the solar neighbourhood, yielding $N_{Ia}/N_{II} \sim 0.2$–0.25 for the LMC and ~ 0.3 for the SMC (Table 4). This is supported by *ASCA* observations of LMC supernova remnants, which can distinguish betweeen the remnants of SNe Ia and SNe II from the X-ray spectra, and which show that the ratio of the rates of SNe Ia to SNe II+Ib in the LMC is as high as 0.25 (Hughes et al. 1995). This implies that the star formation history in the MCs is quite different from that for the solar neighbourhood. As the available chemical data are too limited to constrain unambiguously the star formation history, we have considered two possible scenarios, namely whether stars are formed continuously or as a burst in the MCs. One of our major findings here is that the MCs are characterized by a steepened IMF, almost independently of star formation scenarios considered, unless a galactic wind after a starburst could have very efficiently removed the SNII products from the MCs. This result is supported by recent observations of the MC IMFs (Hill, Madore & Freedman 1994).

The evolutionary behaviour in the continuous star formation model is considerably different from the starburst model, and the difference shows up in the [O/Fe] versus [Fe/H] diagram, the age–metallicity relation, and the present O and Fe abundance distributions of stars (see Figs 9 and 10). Thus, the acquisition of new data, particularly chemical abundances for metal-poor LMC and SMC stars, is strongly recommended for a better understanding of the chemical evolution of the MCs.

ACKNOWLEDGMENTS

We would like to thank T. Shigeyama for useful discussions. This work has been supported in part by the grant-in-Aid for Scientific Research (05242102, 06233101, 07740194, 07804013) and COE research (07CE2002) of the Ministry of Education, Science and Culture in Japan and the Swiss Nationalfonds.

REFERENCES

Anders E., Grevesse N., 1989, Geochim. Cosmochim. Acta, 53, 197
Arnett W. D., 1978, ApJ, 166, 153
Arnett W. D., Schramm D. N., Truran J. W., 1989, ApJ, 339, L27
Barbuy B., 1988, A&A, 191, 121
Barbuy B., Erderlyi-Mendes M., 1989, A&A, 214, 239
Branch D., Nomoto K., Filippenko A. V., 1991, Comments Astrophys., 15, 221
Da Costa G. S., 1990, in Haynes R., Milne D., eds, Proc. IAU Symp. 148, The Magellanic Clouds. Kluwer, Dordrecht, p. 183
Edvardsson B., Andersen J., Gustafsson B., Lambert D. L., Nissen P. E., Tomkin J., 1993, A&A, 275, 101
Gallagher J. S., Hunter D. A., Tutukov A. V., 1984, ApJ, 284, 544
Gilmore G., Wyse R. F. G., 1991, ApJ, 367, L55
Gratton R. G., 1991, in Michaud G. et al., eds, Proc. IAU Symp. 145, Evolution of Stars: The Photospheric abundance Connection. University of Montreal, p. 27, p. 159
Hashimoto M., Nomoto K., Shigeyama T., 1989, A&A, 210, L5
Hashimoto M., Nomoto K., Tsujimoto T., Thielemann F.-K., 1993a, in Käppeler K., ed., Nuclei in the Cosmos. IOP, Bristol, p. 587
Hashimoto M., Iwamoto K., Nomoto K., 1993b, ApJ, 414, L105
Hashimoto M., Nomoto K., Tsujimoto T., Thielemann F.-K., 1994, in McCray T., ed., Proc. IAU Colloq. 145, Supernovae and Supernova Remnants. Cambridge Univ. Press, Cambridge, in press
Hill R. J., Madore B. F., Freedman W. L., 1994, ApJ, 429, 204
Hughes J. P. et al., 1995, ApJ, 444, L81
Matteucci F., 1991b, in Danziger I. J., Kjär K., eds, ESO/EIPC Workshop on Supernova 1987A and other Supernovae. ESO, Garching, p. 703
Matteucci F., François P., 1989, MNRAS, 239, 885
Matteucci F., Greggio L., 1986, A&A, 154, 279
Matteucci F., 1991a, in Lambert D. L., ed., Frontiers of Stellar Evolution, ASP Conf. Ser., Vol. 20, p. 539
Nissen P. E., Edvardsson B., 1992, A&A, 261, 255
Nomoto K., Hashimoto M., 1988, Phys. Rep., 163, 13
Nomoto K., Thielemann F.-K., Wheeler J. C., 1984a, ApJ, 279, L23
Nomoto K., Thielemann F.-K., Yokoi K., 1984b, ApJ, 286, 644
Nomoto K., Shigeyama T., Yanagida S., Hayakawa S., Yasuda K., 1990, in Ferrini F. et al., eds, Chemical and dynamical evolution of galaxies. ETS Editrice, Pisa, p. 366
Nomoto K., Shigeyama T., Tsujimoto T., 1991, in Michaud G., Tutukov A., eds, Proc. IAU Symp. 145, Evolution of Stars: the Photospheric Abundance Connection. Kluwer, Dordrecht, p. 21
Pagel B. E. J., 1992, in Klare G., ed., New Aspects of Magellanic Cloud Research. Springer-Verlag, Berlin
Prantzos N., Hashimoto M., Nomoto K., 1990, A&A, 234, 211
Raiteri C. M., Gallino R., Busso M., Neuberger D., Käppeler F., 1993, ApJ, 419, 207
Russell S. C., Bessell M. S., 1989, ApJS, 70, 865
Russell S. C., Dopita M. A., 1990, ApJS, 74, 93
Russell S. C., Dopita M. A., 1992, ApJ, 384, 508
Tammann G. A., 1993, in Susuki Y., Nakamura Y., eds, Frontiers of Neutrino Astrophysics. Universal Academy Press, Tokyo, p. 255
Thielemann F.-K., Nomoto K., Yokoi K., 1986, A&A, 158, 17
Thielemann F.-K., Nomoto K., Hashimoto M., 1990, ApJ, 349, 222
Thielemann F.-K., Nomoto K., Hashimoto M., 1993, in Prantzos N., Vangoni-Flam E., eds, Origin and Evolution of the Elements. Cambridge Univ. Press, Cambridge, p. 297
Thielemann F.-K., Nomoto K., Hashimoto M., 1994, in Audouze J., Bludman S., Mochkovitch R., Zinn-Justin J., eds, Supernovae, Les Houches, Session LIV. Elsevier, Amsterdam, p. 629
Thielemann F.-K., Nomoto K., Hashimoto M., 1995, ApJ, in press
Tinsley B. M., 1980, Fundam. Cosmic Phys., 5, 287
Tsujimoto T., Nomoto K., Hashimoto M., Thielemann F.-K., 1994, in Sato K., ed., Evolution of the Universe and its Observational Quest. Universal Academy Press, Tokyo, p. 553
Tsujimoto T., Nomoto K., Hashimoto M., Thielemann F.-K., 1995, ApJ, submitted
van den Bergh S., Tammann G. A., 1991, ARA&A, 29, 363
Woosley S. E., Weaver T. A., 1986, Lecture Notes in Phys., 255, 91
Yanagida S., Nomoto K., Hayakawa S., 1990, in Proc. 21st International Cosmic Ray Conference, 4, 44
Yoshii Y., Tsujimoto T., Nomoto K., 1995, ApJ, submitted
Young J. S., Scoville N. Z., 1991, ARA&A, 29, 581